An alternative parameterization of eddy diffusivity in the Gulf of Finland based on the kinetic energy of high frequency internal wave band

Madis-Jaak Lilover[1] and Adolf Konrad Stips[2]

[1] Tallinn University of Technology, Marine Systems Institute, Akadeemia tee 21, EE-12618 Tallinn, Estonia (madis@phys.sea.ee)

[2] European Commission — Joint Research Centre, Institute for Environment and Sustainability, Global Environment Monitoring Unit (TP272), Via E. Fermi 2749, I-21027 Ispra (VA), Italy

In July 1998, three time series of shear microstructure measurements (duration 13, 24 and 14 h, respectively) were performed in 3 different wind-forcing regimes as well as in 3 different background density stratification and current velocity shear situations at the entrance to the Gulf of Finland. We compared the "measured" eddy diffusivities with the diffusivities parameterized using the Richardson number, the Brunt-Väisälä frequency and with the diffusivities simulated using the two-equation k-ε turbulence closure. Summing up the discrepancy of all three time series, the methods applied resulted in a remarkable and consistent bias against the measured eddy diffusivity. Contrary to this result, the calculations with the new suggested parameterization scheme, which accounts for the internal wave kinetic energy of the super-inertial frequency band, fitted well for all three time series. Similarly, the modified k-ε simulations accounting for the super-inertial internal wave energy matched better the measured profiles.

Introduction

The Baltic Sea is a brackish, semi-enclosed sea having a very limited water exchange with the more saline North Sea. The limited water exchange and large river runoff lead to a two-layer salinity stratification with a perennial halocline located at about 60–70 meters below the sea surface. The Gulf of Finland is a typical estuarine environment: the salinity in the surface layer ranges from approximately 5–7 PSU at the entrance to nearly fresh water in the eastern end of the gulf. The general circulation is cyclonic in the gulf and varies strongly due to the wind

forcing (Palmen 1930). Inertial oscillations and seiches are also an important part of the non-stationary circulation pattern (Alenius *et al.* 1998). The tidal oscillations of the sea level have minor importance to the dynamics of the Baltic (Feistel *et al.* 2008). The seasonal thermocline is strongest in July–August and is usually observed at the depth of 10–20 m restricting effectively the nutrient transport to the euphotic layer in summer.

In the last years, biological phenomena like biodiversity or algae blooms were commonly studied in relation to meso- and small-scale physical processes. Biologists are especially
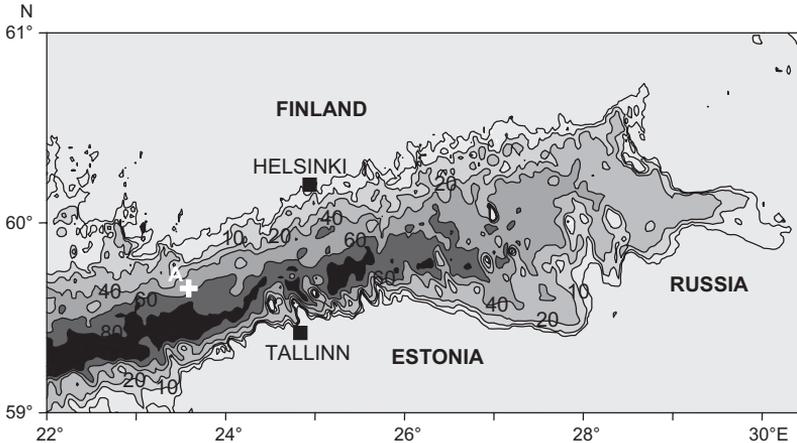
Fig. 1. Locations of the dissipation time series measurements onboard r/v *Aranda* (A and white cross) and of the moored ADCP at the entrance of the Gulf of Finland. Depth contours are given in meters.

interested in estimating the eddy diffusivity to calculate the vertical fluxes of nutrients. Therefore, in interdisciplinary campaigns in addition to the biochemical parameters, also physical parameters like wind, currents, temperature, salinity, density of water and, as a new parameter, turbulent kinetic energy dissipation rate are measured to estimate the eddy diffusivity. Alternatively, the eddy diffusivity can be estimated using parameterization or turbulence modeling. Parameterization schemes relying on the gradients of mean water density and current velocity (using the Richardson number for parameterization) as well as the simulation via the two-equation k-ε turbulence model were usually calibrated for multiannual simulations. Both schemes applied to the Baltic Sea have satisfactorily reproduced the temporal development of the seasonal thermocline (Meier 2001). However, marine biology phenomena, like algae blooms, are sensitive to the nutrient transfer events from the deep water into the euphotic layer (Kononen *et al*. 2003, Lilover *et al*. 2003). Therefore, the turbulent mixing calculation schemes used to explain the marine biology phenomena must be able to reproduce short term mixing events (of about 1 day duration), which can cause significant nutrient pulses into the euphotic zone (Lilover *et al*. 2003).

In the present paper, we focus on the restrictions and capability of different eddy diffusivity calculation schemes to follow short-term forcing changes. Our study is based on three measurement series conducted under different forcing situations. We compare the eddy dif-

fusivities estimated from turbulence measurements, from different parameterization schemes and from the one-dimensional General Ocean Turbulence Model (GOTM, www.gotm.net). We focus on comprehending the turbulence mixing far from the boundaries, i.e. in the stratified "mid-column", where internal waves could play an important role in generating the turbulent fluxes. Finally, we suggest a new scheme for the eddy diffusivity parameterization relying on the high frequency constituent of the current kinetic energy which is able to describe correctly the observed different levels of turbulence. We also suggest a new scheme for incorporation of the turbulence generated by internal waves into the k-ε model for the eddy diffusivity simulation.

Material and methods

The measurements were conducted aboard r/v *Aranda* (Finnish Institute of Marine Research) from 13 to 23 July 1998 at the entrance area to the Gulf of Finland (Fig. 1). The data discussed further were gathered at an anchor station A (59°42.5´N, 23°38.0´E). The basic data-set includes current velocity recorded by a bottom mounted Acoustic Doppler Current Profiler (ADCP) (14–23 July); conductivity, temperature, depth (CTD) and turbulence data collected by a microstructure measuring system (MSS) at anchor stations (A1–A3) on 14–15 (A1), 16–17 (A2) and 21 July (A3). In addition, the wind data at 10-m height with time interval 10 min were extracted from the r/v *Aranda* weather station data file.

The bottom-mounted (at 51 m depth) ADCP (RDI Narrow Band 600 kHz) was deployed by Pirkanmaa Regional Environmental Centre (Finland). The mooring position was chosen as close to the anchor station as possible (about 0.7 km south from the anchor station). The bin size of 1 m and the averaging time interval of 15 min (530 single pings per ensemble) were selected to obtain the accuracy of about 0.01 m s^{-1} for the velocity data from 47 to 7 m depths.

The measurement series with the MSS profiler were conducted on an hourly basis i.e. sub-series consisted of six consecutive profiles per hour. The MSS profiler was equipped with CTD sensors to obtain high-resolution temperature, salinity, density profiles and with a shear probe (time constant approx. 3 ms) to measure current velocity fluctuations (Prandke and Stips 1998). From the latter, the viscous dissipation rate of turbulent kinetic energy, ε ($\varepsilon = 7.5\nu <(\partial u'/\partial z)^2>$, where ν is the kinematic viscosity, $\partial u'/\partial z$ is the vertical profile of current shear fluctuations and $<>$ denote averaging) was calculated with a relative error of about 30% as detailed in Prandke and Stips (1998). The data were sampled at the frequency of 1024 Hz. To avoid cable-induced disturbances the data were collected in freely sinking mode within depths of 5 to 55 m with the mean sinking speed of 0.6 m s^{-1}. However, to avoid possible disturbances by the ship (although the ship was anchored by three anchors and the engine switched off), the turbulence data only from below 7 m were taken into account. This uppermost limit depth follows from the r/v *Aranda* draft of 5 m and from the expert analysis of the raw microstructure data.

The ADCP provided data are the weakest "link" in the hydrophysical data set. Due to the backscatter conditions the ADCP measurements could be noisier than stated in the manual. Further, to consider together the stratification, current velocity and turbulence parameters all measured data have to be filtered the same way. The uniform filtering ensures the coinciding time and space scales resolved by the treated data. For these reasons the ADCP current data were subjected to the spectral analysis to determine the time and vertical space scales for the low-pass filter cutoffs. The rotary spectra of the current velocity components indicated that the white noise would be removed from the series at the filter cutoff value of 2 hours in time domain and at the filter cutoff of 4 meters in vertical space domain. Therefore, to reduce the inherent noise and ensure the comparability (turbulence data resolution in time was 1 hour and the current data resolution in vertical direction was 1 meter), all small- and meso-scale resolving data sets were merged onto 1 m × 1 h grid and then filtered by a low-pass Butterworth filter (Butterworth 1930) with 4 m cut-off in vertical direction and 2 h cut-off in time.

Results and discussion

Wind forcing, background stratification and currents

Considering the wind speed the microstructure measurements were performed under three different wind forcing conditions: rising strong wind (A1), decreasing weak wind (A2) and decreasing strong wind (A3) (Fig. 2). The clockwise rotating spectrum of ADCP velocities revealed a spectral peak at the local inertial frequency (local inertial period is 13.9 h) (Fig. 3). For the further analysis, to consider the contribution of different physical processes which are acting in different frequency bands the fifth-order Butterworth band pass filter was used to divide the current velocity into 3 frequency bands: sub-inertial (< 1.33 cpd (cycles per day)), inertial (1.33–2.4 cpd) and super-inertial (2.4–12 cpd) (Fig. 3). In the layer below the thermocline (the "midcolumn" is our focus) the series' mean kinetic energy and the velocity shear ($s = [(\partial u/\partial z)^2 + (\partial v/\partial z)^2]^{1/2}$) behaved in accordance with the mean wind stress: the highest values belonged to A1 and the lowest to A2 (Table 1). However, the series A3 had the highest inertial and superinertial frequency band kinetic energy and the series A2 the lowest.

For the entire measurement period the sub-inertial current velocity shear was strongest in the upper layer. Below the thermocline the inertial shear prevailed during the entire current velocity measurement period. The mean stratification was influenced by the meso-scale flow and weakened continuously from A1 toward A3
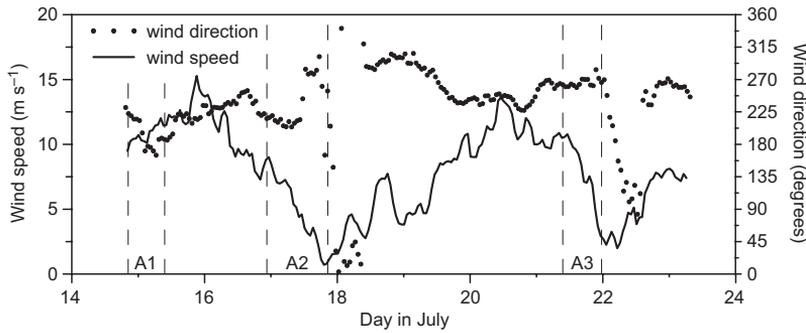
Fig. 2. Two-hour average wind speed and direction during the measurement period. Time series A1, A2 and A3 are marked by vertical dashed lines.
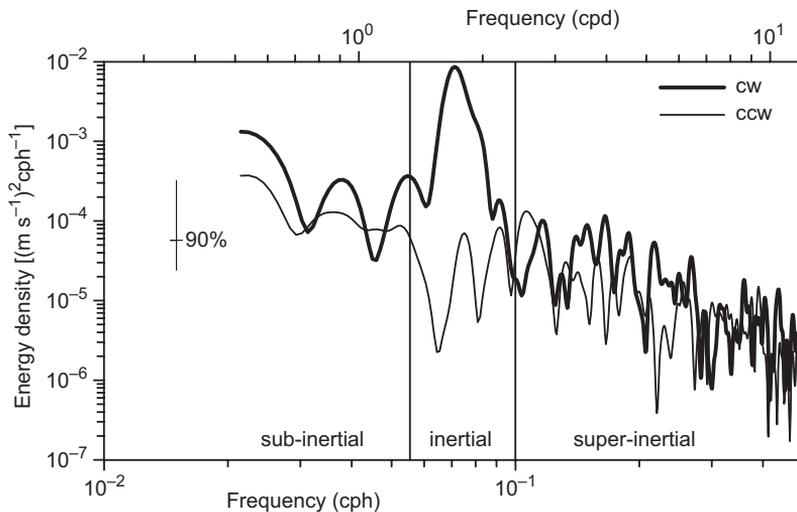

Fig. 3. Rotary spectra of the 9 days ADCP velocity at the 30-m depth. Thick and thin lines indicated clockwise and counterclockwise spectra, respectively. The division into sub-frequency bands (sub-inertial, inertial and super-inertial) is indicated by vertical lines. Vertical error bar shows the 90% confidence level.

— during series A3 the stratification was the weakest (Fig. 4). Thus, in terms of generation of turbulence, in case of A2 the mixing could presumably have been developed weakly because of the weakest wind forcing, the weakest shear and medium stratification. In case of A1, a more intensive mixing is expected because of the strong shear caused by strong wind forcing. In case of A3, the weak stratification and relatively strong shear could have been hypothetical factors supporting the turbulent mixing. In the latter case, the relative contribution to the velocity shear from the super-inertial frequency band was the largest.

Table 1. Mean characteristics of wind, current kinetic energy, vertical shear and buoyancy frequency in the water column below the thermocline (from 20 to 47 m depth) during the three time series.

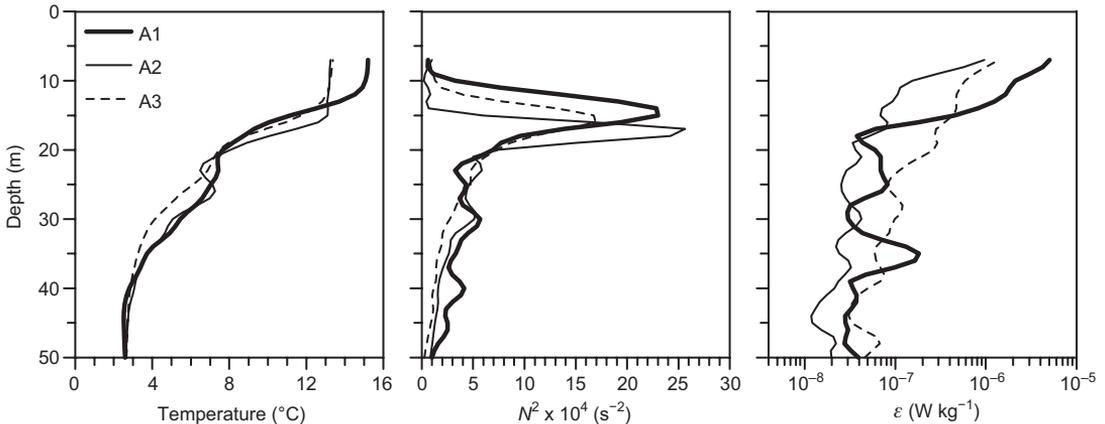|	A1	A2	A3
Wind speed (m s^{-1})	11	5	8
Wind stress (N m^{-2})	0.20	0.04	0.10
Kinetic energy (10^{-4} J kg^{-1})	62.3	11.3	53.5
Sub-inertial kinetic energy (10^{-4} J kg^{-1})	46.6	8.0	33.2
Inertial kinetic energy (10^{-4} J kg^{-1})	14.7	2.7	18.4
Super-inertial kinetic energy (10^{-4} J kg^{-1})	1.0	0.6	1.9
Shear squared (s^2) (10^{-4} s^{-2})	1.3	0.8	1.0
Sub-inertial shear squared (10^{-4} s^{-2})	0.4	0.2	0.3
Inertial shear squared (10^{-4} s^{-2})	0.6	0.3	0.3
Super-inertial shear squared (10^{-4} s^{-2})	0.3	0.3	0.4
Buoyancy frequency squared (N^2) (10^{-4} s^{-2})	3.3	2.7	1.9

Fig. 4. Average profiles of temperature, squared buoyancy frequency and "measured" dissipation rate for time series A1, A2 and A3.

Dissipation profiles

Three time-averaged profiles of kinetic energy dissipation rate ε of time series A1, A2 and A3 have common features as well as some peculiarities (Fig. 4). From the ε profiles we can summarize the common features as follows: (1) ε has large values in the layer above the pycnocline (thermocline); (2) in the uppermost part of this layer ε behaved in accordance with the wind stress; (3) in the lower layer ε values are up to about one decade smaller than in the upper layer. The most pronounced peculiarity is that the value of ε below the pycnocline is about 3 times larger in A3 than in the reference case A2 (case A2 represents the dissipation and the eddy diffusivity during "calm" weather therefore here and hereafter A2 will be referred to as reference case).

"Measured" eddy diffusivity (Osborn model)

The vertical eddy diffusivity of mass calculated from the measured quantities (ε, N^2) was estimated from the Osborn (1980) model with $K_\rho = 0.2\varepsilon/N^2$, where N^2 ($N^2 = -g\rho^{-1}\partial\rho/\partial z$, where g is the gravitational acceleration and ρ is water density) is the buoyancy frequency squared. The used constant mixing efficiency of 0.2 is subject to debate, though it generally represents a good choice for stationary flow in weak stratification (Shih *et al.* 2005). This has been

further supported by several concurrent tracer and dissipation measurement studies (Ledwell *et al.* 1998, Oakey and Greenan 2004). Also Lass *et al.* (2003) reported that in the Baltic Sea the dissipation-based diffusivity estimates (Osborn model with the mixing efficiency 0.2) agreed well with the averaged value obtained from measurements of dispersion of dye tracers released in the thermocline and halocline of the Arkona and Bornholm basins (Kullenberg 1977). The model assumes a local production–dissipation balance of the turbulent kinetic energy and therefore the eddy diffusivity was calculated for the layer below the maximum of the buoyancy frequency where we assume the Osborn model applies. Because of the small-scale turbulence intermittency the mean eddy diffusivity profiles were calculated from the individual profiles (henceforth K_ρ denotes the mean eddy diffusivity). Below the upper mixed layer (UML) the mean eddy diffusivity profile remained moderately variable within the range of 10^{-5}–10^{-4} m^2 s^{-1} (Fig. 5a). However, in that layer all three mean profiles corresponding to cases A1, A2 and A3 were significantly shifted relative to each other. Compared with the weakest level of turbulence in case of A2, a larger K_ρ was observed in A1 probably due to the strong current shear and in A3 probably due to the relatively strong shear and the weakest stratification (Table 1). So, the "measured" eddy diffusivities presented here clearly reflect the changes in the background fields' characteristics.
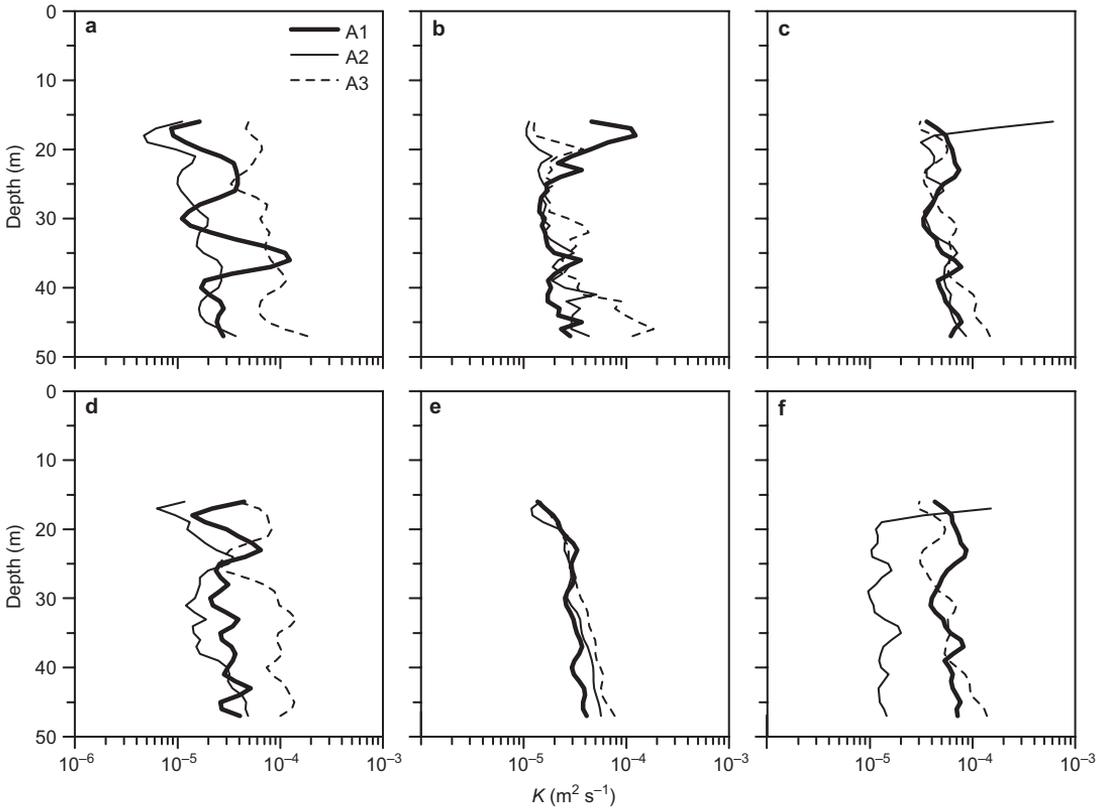
Fig. 5. (**a**) Average profiles of "measured" eddy diffusivity (K_ρ), (**b**) parameterized using Pacanowski and Philander (1981) scheme (K_{Pac}), (**c**) simulated by a standard k-ε model ($K_{k-\varepsilon}$), (**d**) parameterized using the new scheme (K_{supi}), (**e**) parameterized using scheme $K = a_0 N^{-1}$, and (**f**) simulated using the new scheme ($K_{k-\varepsilon\,supi}$).

Further we assess the skill of different parameterization schemes to distinguish the time series under consideration.

Parameterization of eddy diffusivity in the form $K_{Ri} = f(Ri)$

Next we discuss the approximation of eddy diffusivity using Richardson number (Ri = N^2/s^2) dependent parameterization scheme. The formula is adopted from Pacanowski and Philander (1981) and Meier (2001):

$$K_{Meier,\,Pac} = K_0/(1 + Ri/Ri_0)^q + K_b \qquad (1)$$

where except Ri all quantities are constants given in Table 2. The scheme by Pacanovski and Philander (Pac) has been developed for the equatorial Pacific Ocean and the scheme developed by Meier for the Baltic Sea. Both schemes were verified with modeled data. Actually the values of constants of these two schemes were estimated for a large area and for a long simulation time therefore the estimated values are not location specific but rather region specific (Equatorial Pacific Ocean, Baltic Sea). The Ri dependent

Table 2. Constants of the Richardson number dependent turbulent mixing parameterization.

	$K_0 \times 10^{-4}$ (m² s⁻¹)	$K_b \times 10^{-4}$ (m² s⁻¹)	q	Ri_0	
K_{Meier}	20	0.01	1.5	0.1	Meier (2001)
K_{Pac}	$50(1 + Ri/Ri_0)^{-2} + 1$	0.1	1	0.2	Pacanowski and Philander (1981)

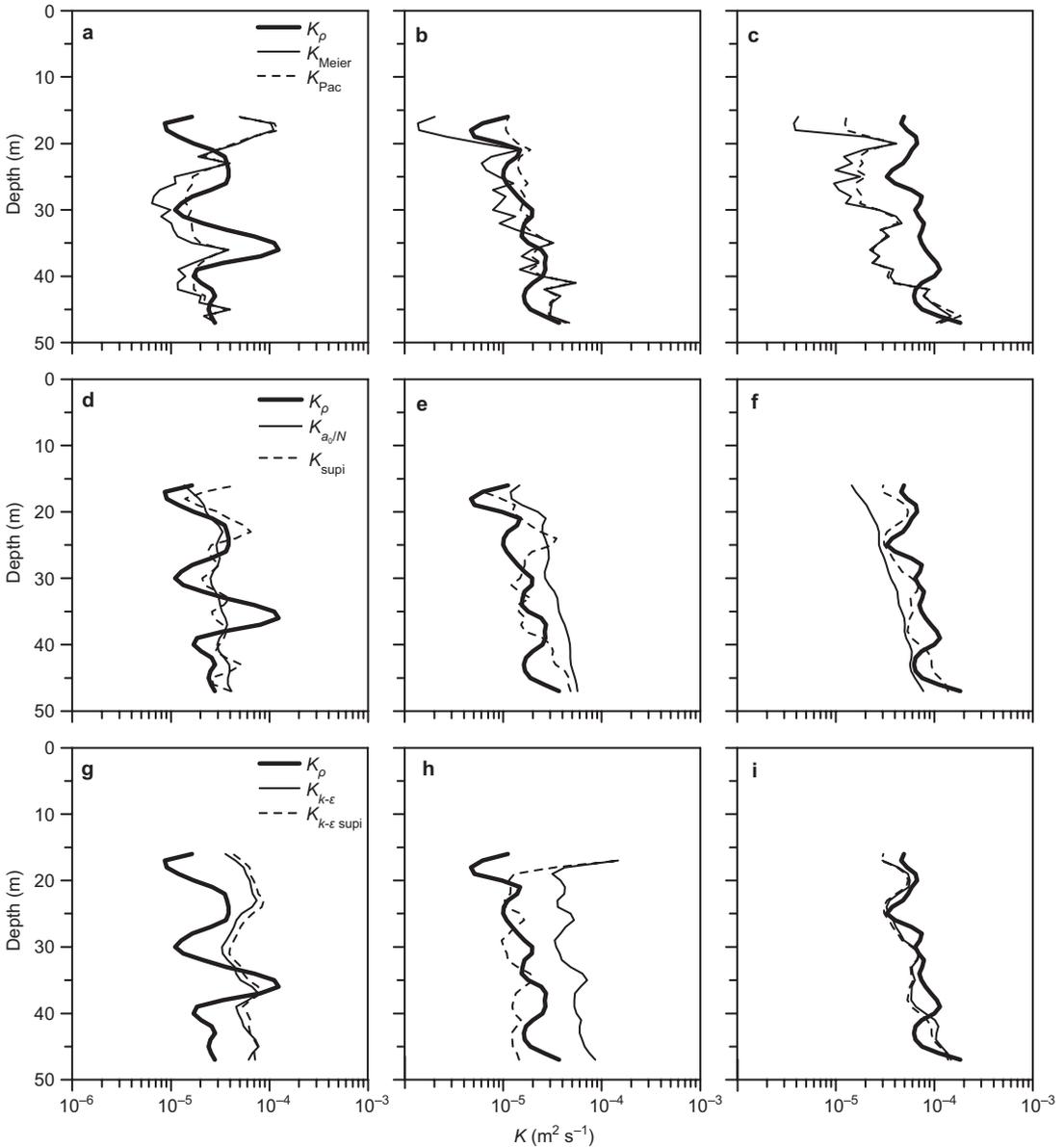**Fig. 6**. (**a–c**) Time mean profiles of "measured" eddy diffusivity (K_ρ) for three time series A1, A2 and A3, respectively, compared with profiles of parameterization using Pacanowski and Philander (1981) (K_{Pac}) and Meier (2001) (K_{Meier}) schemes. (**d–f**) Profiles of parameterization using Eq. 2 ($K_{a_0/N}$) and the new scheme (K_{supi}) for three time series A1, A2 and A3, respectively. (**g–i**) Profiles simulated by the standard ($K_{k\text{-}\varepsilon}$) and the new ($K_{k\text{-}\varepsilon\ supi}$) $k\text{-}\varepsilon$ models for three time series A1, A2 and A3, respectively.

parameterized vertical profiles of the eddy diffusivity fit better in case A2 and are obviously too small in case A3 (Fig. 6a–c). These parameterizations fail to some extent in the lower part of thermocline (layer 15–20 m) in all three time series. The fit in the layer below (20–47 m) can be characterized in the following way: (1) in case

A1, K_{Meier} nicely follows the changes in depth but is shifted to smaller values; (2) in case A2, both K_{Meier} and K_{Pac} fit quite well; (3) in case A3, both K_{Meier} and K_{Pac} are strongly shifted towards smaller values. Relying on the series mean vertical profiles (Fig. 6a–c) we can summarize here that in our measurements at the entrance of the
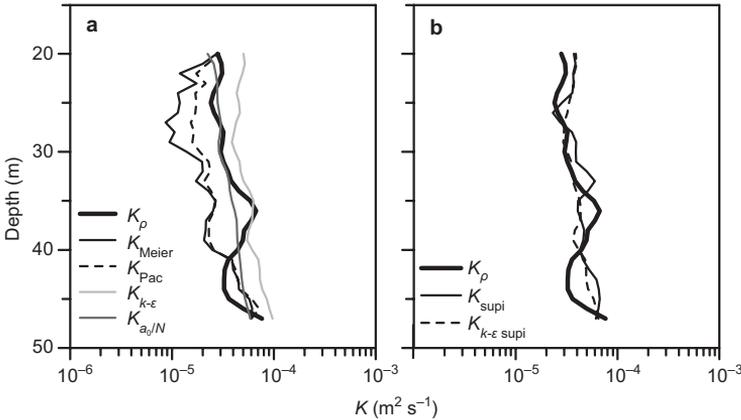
Fig. 7. (**a**) Campaign average "measured" eddy diffusivity profile (K_ρ), profiles of parameterization using Meier (2001) (K_{Meier}), Pacanowski and Philander (1981) (K_{Pac}) and Eq. 2 ($K_{a_0/N}$) schemes and profile of parameterization simulated by the standard k-ε model ($K_{k-\varepsilon}$). (**b**) Campaign average "measured" eddy diffusivity profile (K_ρ), profile of parameterization using the new scheme (K_{supi}) and profile simulated by using the new scheme ($K_{k-\varepsilon\ supi}$).

Gulf of Finland the parameterization scheme by Meier is more sensitive to Ri changes but the deviation from the measured data is larger than for the Pacanovski and Philander scheme. However, both these parameterization schemes are not able to describe the mean measured profiles for all three time series — namely A3 has 4–5 times larger bias than A1 and A2 (Fig. 5b). Thus, we must continue to seek a parameterization and/or simulation scheme which will describe all three time series equally well.

Eddy diffusivity simulated by the standard *k-ε* model

We simulated the eddy diffusivity (Fig. 6g–i) using a two-equation k-ε turbulence closure from the GOTM model. Different modeling scenarios were tested, applying either only meteorological forcing or additional forcing by measured current velocities. It was necessary to relax the simulated temperature and salinity to the measured ones, because the advective processes were important in that area. In the sensitivity study the minimum turbulent kinetic energy (TKE_{min}) as the model tuning parameter representing all not accounted in the model turbulence generation processes was adapted to achieve the minimal bias of the energy dissipation rate. Nevertheless, it was not possible to obtain a good reproduction of the eddy diffusivity for all three time series using only one simulation constant TKE_{min}. The adjustment of simulated values to the measured reference time series A2 resulted in a large bias for time series A3 and vice versa,

adjusting the model values to the time series A3 produced large biases for A1 and A2 (Fig. 6g–i, $K_{k-\varepsilon}$). Therefore, in our case the applied standard k-ε model (GOTM), like the parameterization schemes described above, failed simulating equally well all three time series (or, in other words, failed separating time series with diverse mean values or proved to be insufficiently "sensitive") (Fig. 5c).

Comparison of the campaign-averaged time series profiles

The models (and model constants) presented above had been obtained for long-term modeling of ocean mean temperature, salinity and current fields. Therefore, we can expect better coincidence for the mean time series profiles averaged over the entire campaign period comprising 49 hours of measurements during 8 days. Besides the "sensitivity" problem discovered above, the campaign mean eddy diffusivities revealed some bias relative to the measured average profile (Fig. 7a). Namely, both parameterized averaged profiles had smaller and the k-ε model results larger values than the measured mean.

Alternative parameterization of eddy diffusivity

It is common for the tested parameterization schemes and models that they are relying on the resolved mean current velocity shear and do not take into account high frequency break-

ing internal waves as an additional source of turbulence. Alternatively, considering the internal waves breaking in the deep ocean (Gargett 1984, Gargett and Holloway 1984) as well as in the Baltic Sea (Stigebrandt 1987) the following parameterization of eddy diffusivity

$$K = a_0 N^{-1} \qquad (2)$$

with constant a_0 was successfully used. Our three measured series have three different mean values of N. Still, parameterization (Eq. 2) does not provide the order of the time series because A2 has the smallest mean measured K_ρ but not the largest N to rank the parameterized K to the order of measured K_ρ (Fig. 5e). Therefore, the latter scheme (Eq. 2) with a constant a_0 value is not suitable to separate the time series with diverse mean eddy diffusivity values. However, it was proposed (Stigebrandt 1995, Axell 1998) that a_0 could be regarded as not constant but rather

depending on energy fluxes of local sources. Accordingly, for a_0 different constant values and parameterization formulas could be found in the literature (Table 3). As our measurement site location in the Gulf of Finland is in a sense similar to the location of BY31 in the Landsort Deep within the coastal boundary layer, we chose $a_0 = 6 \times 10^{-7}$ m^2 s^{-2} as it was estimated for the Landsort Deep (Table 3). The corresponding campaign mean parameterized profile (Eq. 2) and the measured profile coincide reasonably well (Fig. 7a). Despite of this general good coincidence there remains the problem of describing the time dependence of a_0 to ensure the sufficient "sensitivity" of the scheme.

Axell (2002) speculated about the physical interpretation of a_0 in Eq. 2 and found that combining the Osborn (1980) model for the eddy diffusivity ($K \propto \varepsilon N^{-2}$) and the common turbulence scaling [$K \propto k^2 \varepsilon^{-1}$ (Rodi 1980)] the eddy diffusivity should scale as

Table 3. Scaling parameter a_0 values from the literature and in our study.

$a_0 \times 10^{-7}$ (m^2 s^{-2})	Location and method	Constant or variable	Reference
1	Ocean	constant	Gargett (1984)
2.0	Baltic Proper, climatological mean, comparison of simulated *versus* observed stratification	constant	Stigebrandt (1987)
1.5	Gotland Deep, BY15, annual mean, budget method	Seasonally variable energy according to the wind	Axell (1998)
6	Landsort Deep, BY31, annual mean, budget method	Seasonally variable according to the high-energetic coastal processes	Axell (1998)
0.5–1.0	Gotland Deep, 14 years simulation, comparison of extended k-ε model salinity *versus* measured salinity	constant	Meier (2001)
0.87	Gotland Basin, 9-day mean, comparison versus measured K_ρ	constant	Lass *et al.* (2003)
$\alpha(E_{kin} + E_{pot})$	Gotland Basin, 9-day mean, comparison *versus* measured K_ρ	Variable according to the total energy of internal waves	Lass *et al.* (2003)
6	Entrance to the Gulf of Finland, 49-hour mean, comparison *versus* measured K_ρ	constant	this paper
$\gamma E_{kin.supi}$	Entrance to the Gulf of Finland; 13-, 22- and 14-hour time series mean, comparison *versus* measured K_ρ	Variable according to the super-inertial waves kinetic energy	this paper
7	Entrance to the Gulf of Finland; 9-day mean of $\gamma E_{kin.supi}$	Variable according to the super-inertial waves kinetic energy	this paper

$$K \propto kN^{-1} \tag{3}$$

where k denotes the turbulent kinetic energy (TKE) density. Relying on Eqs. 2 and 3 Axell (2002) concluded that a_0 could be related to the mean background level of the TKE due to unresolved shear resulting from the direct input of wind energy. A similar attempt to connect a_0, estimated from our data, with the wind energy was unsuccessful. Also Lass *et al.* (2003) found that turbulence below the surface layer is not directly related to the surface forcing. Based on the dissipation rate profiles measured in the Baltic Proper Lass *et al.* (2003) proposed that a_0 could be proportional to the total energy of internal waves, $a_0 = \alpha(E_{kin} + E_{pot})$, where E_{kin} and E_{pot} are the average profiles of the kinetic and the potential energy densities of the internal wave field and α is a dimensionless constant. While estimating E_{kin} from current meter records the energy of the inertial oscillation was removed. This parameterization agreed well below but was unsatisfactory above 60 meters depth (upper rim of halocline).

Our trial to describe the time evolution of a_0 using the internal wave kinetic energy similar to Lass *et al.* (2003) failed also. Therefore, we assumed that the internal wave energy in the inertial frequency band masks the contribution of the higher frequency internal waves to the turbulence and we suggest to consider only the super-inertial part of the internal wave kinetic energy for the parameterization. Unlike our proposal in Lass *et al.* (2003) the inertial band internal wave energy was taken into account for the parameterization (only the inertial oscillation kinetic energy was removed). Hence, we propose to parameterize the eddy diffusivity using the following equation:

$$K_{supi} = \gamma E_{kin.supi} N^{-1} \tag{4}$$

which is similar to Eqs. 2 and 3, where $a_0 = \gamma E_{kin.supi}$, $E_{kin.supi}$ being the kinetic energy of internal waves with frequencies higher than the inertial frequency and γ is a dimensionless constant. This parameterization separates series A1 and A3 from A2 correctly (Fig. 5d) and provides vertical diffusivity profiles reasonably similar to the measured eddy diffusivity (Fig. 6d–f). To evaluate the prognostic skill of the model, the parameter γ was calculated for time series A3 only ($\gamma = 0.0063$) and this value was further applied to time series A1 and A2 (the latter explains the smallest bias in case of A3). The same γ value was used to calculate a_0 ($a_0 = 7 \times 10^{-7}$ m^2 s^{-2}, Table 3) for the full (9 days) current velocity measurement period. The latter value is close to our best fit for the 49-hour mean value and to the value found by Axell (1998) for the Landsort Deep. Furthermore, if compared with other methods under consideration, the scheme using Eq. 4 provides the smallest time series average absolute biases and root mean squared differences (Table 4).

Gargett and Holloway (1984) argued that in the ocean a_0 is "constant" within a factor of 2 or 3. According to Table 3 this concept holds for the Baltic Sea region beyond the coastal boundary layer (in the regions of the Baltic Proper and Gotland Deep a_0 varies from 1×10^{-7} to 2×10^{-7} m^2 s^{-2}). In regions not far away from the coast a larger a_0 value has been observed (in Landsort

Table 4. Model performance parameters (layer 20–47 m).

Eddy diffusivity	MoA bias[1] $[1/3(|A1_{bias}| + |A2_{bias}| + |A3_{bias}|)]$	Mean RMSD[2] $[1/3(A1_{RMSD} + A2_{RMSD} + A3_{RMSD})]$	Local production of TKE by
K_{Pac}	0.18	0.28	current shear
K_{Meier}	0.22	0.35	current shear
$K_{k\text{-}\varepsilon}$	0.26	0.32	current shear
$K_{a_0/N}$	0.20	0.28	internal waves
K_{supi}	0.07	0.22	internal waves
$K_{k\text{-}\varepsilon\,supi}$	0.17	0.24	current shear and internal waves

K_{Pac}, K_{Meier}, $K_{a_0/N}$ and K_{supi}: eddy diffusivity parameterization schemes according to (Pacanovski and Philander 1981), (Meier 2001), Eqs. 2 and 4 of the current paper, respectively. $K_{k\text{-}\varepsilon}$ and $K_{k\text{-}\varepsilon\,supi}$: eddy diffusivity simulations by GOTM using the standard setup and using the setup proposed in the current paper, respectively.

Deep and in the entrance to the Gulf of Finland a_0 had the value of 6×10^{-7} m^2 s^{-2}). Axell (1998) assumed that the latter can be explained by a large energy contribution from coastal processes.

Following the above argumentation about the new eddy diffusivity parameterization, we suggest to parameterize the TKE dissipation rate as

$$\varepsilon = \beta E_{kin.supi} N \tag{5}$$

where β is a dimensionless constant. Similar to Eq. 4, the parameterization of the TKE dissipation rate (Eq. 5) using the superinertial band of the internal wave kinetic energy gave good agreement with the measured dissipation rate below the thermocline (not shown). Lass *et al.* (2003) suggested to use the form $\varepsilon = \alpha(E_{kin} + E_{pot})N$, which gave good results below but unsatisfactory above the halocline. For the data collected in the New England shelf area, MacKinnon and Gregg (2003) proposed $\varepsilon = \varepsilon_0(N/N_0)(s/s_0)$. The latter formula applied to our data did not give satisfactory results as the parameterized mean profiles of the TKE dissipation rate for the time series A1, A2 and A3 were not separated in right order.

New simulation of eddy diffusivity

Two-equation turbulence models, such as the k-ε model (Rodi 1987), are widely used to model the eddy viscosity and diffusivity within the water column. These models are usually forced by only surface momentum and buoyancy fluxes. In the mid-column the mean shear is the only turbulence energy source. This type of models has been successfully applied to reproduce turbulence levels in the surface and in the bottom layer (Simpson *et al.* 1996, Stips *et al.* 2002). However, it is also well established that the results of such models deviate from the observed levels of the dissipation rate in and below the pycnocline by several orders of magnitude (Simpson *et al.* 1996, Rippeth 2005). As turbulence generation is based on the available TKE resulting from the buoyancy and resolved current shear, this fact points to a missing source of the TKE in and below the pycnocline. In order to avoid the model predicting unrealistic low dissipation rates at mid-water depth, a lower limit for the TKE is usually introduced (Mellor

1989, Burchard *et al.* 1998). The limit actually introduces an additional crude parameterization of TKE generation by unresolved internal wave breaking. It can be expected that the spatial and temporal variations of the TKE background level really exist, therefore Axell (2002) proposed a modified parameterization. In the latter modified parameterization the lower limit of the TKE (further TKE$_{min}$) is assumed a function of the local wind energy input. It is argued that regardless of the exact nature of the energy generation process the internal wave energy available for deepwater mixing should be correlated with the wind energy. In Axell (2002), the energy flux density from the mixed layer is basically considered to be proportional to the cube of the wind friction velocity. This approach, however, ignores the fact that the internal waves are influenced not only by the local wind velocity, but also by the wind direction changes as well as by the geostrophic adjustment of coastal jets and mesoscale eddies. This argument is actually indirectly supported by Lass *et al.* (2003), who could not find any correlation between the energy dissipation variability in the deeper interior and the local wind velocity fluctuations. Indeed, the respective trial to simulate our measurements using the parameterization according to (Axell 2002) was not successful.

We are, therefore, proposing a different approach, which is in line with the presented above ideas about an additional source of the TKE derived from the super inertial current shear. As stated above the internal waves with frequencies higher than the inertial frequency could be responsible for the explained additional turbulence generation which in particular took place during the time series A3. We, therefore, parameterized this energy in the "mid-column" (excluding the upper mixed layer and bottom layer) by considering the TKE$_{min}$ a function of the vertically averaged super-inertial frequency band kinetic energy. Written in a simplified way this parameterization in our example looks like:

$$\text{TKE}_{min}(t) = \lambda E_{kin.supi(20–45 \text{ m})}(t) \tag{6}$$

where t is the time dependency and the exact value of λ should be determined from observations. For testing our hypothesis we chose λ in such a way that the eddy diffusivity of the

new model would follow as close as possible the eddy diffusivity profiles following from the k-ε and the Osborn models for time series A3 ($\lambda = 0.01$ provided the best fit which showing that in case of A3 at least 1% of the available superinertial kinetic energy might be converted to turbulence). It can be seen (Fig. 6g–i, $K_{k\text{-}\varepsilon \text{ supi}}$) that this new approach explains different levels of dissipation rate and eddy diffusivity qualitatively well. The parametrization applied clearly separates the low level turbulence in case A2 from the other two enhanced turbulence cases A1 and A3 which was not achieved by the other tested standard simulations. Though, the reason of the simulation for A1 being worse than for A2 remains obscure. Possibly the model overestimates the turbulence production for the strong inertial shear in case A1 (Table 1).

Comparison of model performance

To assess quantitatively the ability of the presented schemes to describe equally well mean eddy diffusivity profiles in all three time series we present the mean value of series' absolute biases (MoA bias) and the mean value of series' root mean squared differences (mean RMSD) calculated for logarithmic profiles (Table 4). According to MoA bias and mean RMSD the new parameterization scheme which considers the superinertial waves kinetic energy is the best in estimating the eddy diffusivity under different forcing conditions. Similarly, the modified k-ε simulations, which considered the super-inertial internal wave energy, gave the second smallest overall MoA bias and the mean RMSD value (the smallest from the simulations). As the parameters in the table are computed for log-profiles of eddy diffusivity then e.g. the MoA bias 0.2 means that the model value is 1.5 times larger then the measured K value or, respectively, the MoA bias value 0.3 corresponds to the 3 times larger model value.

Summary and conclusions

It has been often argued that the near-inertial oscillations are the most energetic or at least contribute the most to the squared vertical shear in the Baltic Sea below the upper mixed layer (Krauss 1981). However, the 9-day ADCP current measurements within the CYANO98 experiment revealed that the described picture did not hold at the entrance to the Gulf of Finland with an estuary like stratification and is known as an area of nearly permanent fronts. For the full measurement period (9 days) the subinertial energy (kinetic energy of meso-scale processes) prevailed in the water column. In the layer below the thermocline in the three time series, the average subinertial energy contribution to the total kinetic energy was 69% and to the inertial band energy 28%. Besides these two large energy contributors the super-inertial band energy contribution was about 3% of the total kinetic energy but its distribution appeared to be proportional to the turbulent kinetic energy dissipation rate (not shown). The sub-inertial current velocity vertical shear squared, s^2, dominated in the upper layer while in the layer below the thermocline inertial s^2 prevailed for the full measurement period (9 days). In the latter layer, the three time series average subinertial s^2 contribution to the total s^2 was 26% and to the inertial band s^2 35%. Unlike the superinertial band kinetic energy the superinertial shear squared contributed as much as 29% to the total shear squared. Time series A3 revealing the largest TKE dissipation rate had the largest superinertial energy and shear squared values relative to series A1 and A2.

The measured turbulence parameters followed the wind forcing in the UML but not in the entire water column. In the layer below the thermocline the dissipation rate appeared to be proportional to the product of the super-inertial kinetic energy and the buoyancy frequency (not shown). The parameterizations of the eddy diffusivity as a function of the mean Richardson number or the mean Brunt-Väisälä frequency did not separate the series' mean profiles in the correct order displayed by the measured eddy diffusivity. The parameterization with the new proposed scheme considering the super-inertial internal waves kinetic energy resulted in the right sequence of the mean eddy diffusivity profiles. The modified k-ε simulations taking into account the superinertial band internal waves energy corresponded qualitatively well to the measured profiles.

Finally, compared with parameterizations $K = f(\mathrm{Ri})$ or $K = f(N)$ the new parameterization $K = f(E_{\mathrm{kin.supi}}, N)$ describes the variability of the measured eddy diffusivity better (smaller bias and better "sensitivity"). Also, compared with the standard k-ε model with the constant $\mathrm{TKE}_{\mathrm{min}}$, the $\mathrm{TKE}_{\mathrm{min}}$ parameterization using mean $E_{\mathrm{kin.supi}}$ describes the variability of measured eddy diffusivity better (smaller bias and better "sensitivity").

Still, despite the suggested parameterization scheme is developed on the bases of three quite different data series, considering that the data were measured at the same sea location during one week period a further independent validation (additional dissipation measurements in other situations) is required to judge on the limits of applicability of the suggested parameterization.

References

Alenius P., Myrberg K. & Nekrasov A. 1998. Physical oceanography of the Gulf of Finland: a review. *Boreal Env. Res.* 3: 97–129.

Axell L.B. 1998. On the variability of Baltic Sea deepwater mixing. *J. Geophys. Res.* 103: 21667–21682.

Axell L.B. 2002. Wind-driven internal waves and Langmuir circulations in a numerical ocean model of the southern Baltic Sea. *J. Geophys. Res.* 107: 3204, doi:10.1029/2001JC000922.

Burchard H., Petersen O. & Rippeth T.P. 1998. Comparing the performance of the Mellor-Yamada and the k-ε two-equation turbulence models. *J. Geophys. Res.* 103: 10543–10554.

Butterworth S. 1930. On the theory of filter amplifiers. *Experimental Wireless and the Wireless Engineering* 7: 536–541.

Feistel R., Nausch G. & Wasmund N. 2008. *State and evolution of the Baltic Sea, 1952–2005: a detailed 50-year survey of meteorology and climate, physics, chemistry, biology and marine environment*. John Wiley & Sons, Hoboken, NJ.

Gargett A.E. 1984. Vertical eddy diffusivity in the ocean interior. *J. Mar. Res.* 42: 359–393.

Gargett A.E. & Holloway G. 1984. Dissipation and diffusion by internal wave breaking. *J. Mar. Res.* 42: 15–27.

Kononen K., Huttunen M., Hällfors S., Gentien P., Lunven M., Huttula T., Laanemets J., Lilover M.-J., Pavelson J. & Stips A. 2003. Development of a deep chlorophyll maximum of Heterocapsa triquetra Ehrenb. at the entrance to the Gulf of Finland. *Limnol. Oceanog.* 48: 594–607.

Kullenberg G.E.B. 1977. Observations of the mixing in the Baltic thermo- and halocline layers. *Tellus* 29: 572–587.

Krauss W. 1981. The erosion of a thermocline. *J. Phys. Oceanogr.* 11: 415–453.

Lass H.-U., Prandke H. & Liljebladh B. 2003. Dissipation in the Baltic Proper during winter stratification. *J. Geophys. Res.* 108(C6): 3187, doi:10.102972002JC001401.

Ledwell J.R., Watson A.J. & Law C.S. 1998. Mixing of a tracer in the pycnocline. *J. Geophys. Res.* 103: 21499–21529.

Lilover M.-J., Laanemets J., Kullas T., Stips A. & Kononen K. 2003. Late summer vertical nutrient fluxes estimated from direct turbulence measurements: a Gulf of Finland case study. *Proc. Estonian Acad. Sci. Biol. Ecol.* 52: 193–204.

Mackinnon J.A. & Gregg M.C. 2003. Mixing on the late summer New England shelf — solibores, shear, and stratification. *J. Phys. Oceanogr.* 33: 1476–1492.

Meier H.E.M. 2001. On the parameterization of mixing in three-dimensional Baltic Sea models. *J. Geophus. Res.* 106: 30997–31016.

Mellor G.L. 1989. Retrospect on oceanic boundary layer modelling and second moment closure. In: Henderson D. & Müller P. (eds.), *The parameterization of small-scale processes*, University of Hawaii, Honolulu, pp. 251–271.

Oakey N.S. & Greenan B.J.W. 2004. Mixing in a coastal environment: 2. A view from microstructure measurements. *J. Geophys. Res.* 109: C10014, doi:10.1029/2003JC002193.

Osborn T. 1980. Estimates of the local rate of vertical diffusion from dissipation measurements. *J. Phys. Oceanogr.* 10: 83–89.

Pacanowski R.C. & Philander S.G.H. 1981. Parameterization of vertical mixing in numerical models of tropical oceans. *J. Phys. Oceanogr.* 11: 1443–1451.

Palmén E. 1930. Untersuchungen über die Strömungen in den Finnland umgebenden Meeren. *Soc. Sci. Fenn. Comm. Phys.-Math.* 5(12): 1–94.

Prandke H. & Stips A. 1998. Test measurements with an operational Microstructure-Turbulence profiler: detection limit of dissipation rates. *Aquat. Sci.* 60: 191–209.

Rippeth T.P. 2005. Mixing in seasonally stratified shelf seas: a shifting paradigm. *Phil. Trans. Roy. Soc. London A* 363: 2837–2854.

Rodi W. 1980. *Turbulence models and their application in hydraulics — a state-of-the-art review*. Int. Assoc. for Hydraul. Res., Delft.

Rodi W. 1987. Examples of calculation methods for flow and mixing in stratified flows. *J. Geophys. Res.* 92: 5305–5328.

Shih L.H., Koseff J.R., Ivey G.N. & Ferziger J.H. 2005. Parameterization of turbulent fluxes and scales using

homogeneous sheared stably stratified turbulence simulations. *J. Fluid Mech.* 525: 193–214.

Simpson J.H., Crawford W.R., Rippeth T.P., Campbell A.R. & Choak J.V.S. 1996. Vertical structure of turbulent dissipation in shelf seas. *J. Phys. Oceanogr.* 26: 1580–1590.

Stigebrandt A. 1987. A model for the vertical circulation of the Baltic deep water. *J. Phys. Oceanogr.* 17: 1772–1785.

Stigebrandt A. 1987. A model for the vertical circulation of the Baltic deep water. *J. Phys. Oceanogr.* 17: 1772–1785.

Stigebrandt A. 1995. The large-scale vertical circulation of the Baltic Sea. In: Omstedt A. (ed.), *First Study Conference on BALTEX*, BALTEX Sect., pp. 28–47.

Stips A., Burchard H., Bolding K. & Eifler W. 2002. Modelling of convective turbulence with a two-equation k-ε turbulence closure scheme. *Ocean Dyn.* 52: 153–168.